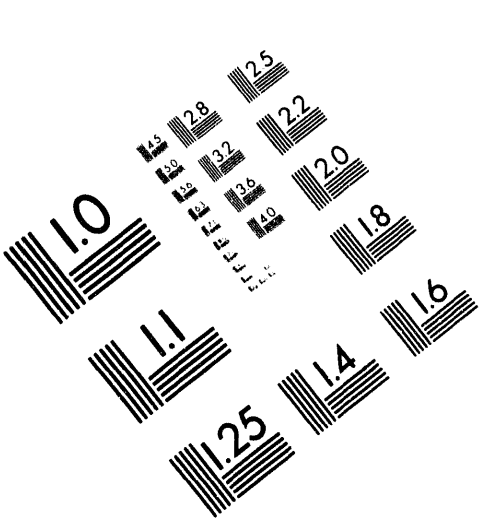

Association for Information and Image Management

1100 Wayne Avenue, Suite 1100
Silver Spring, Maryland 20910

301/587-8202

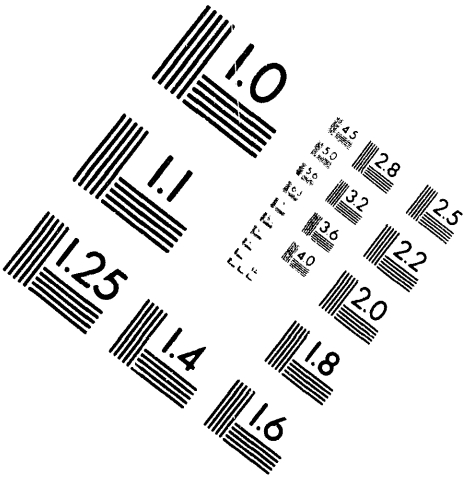

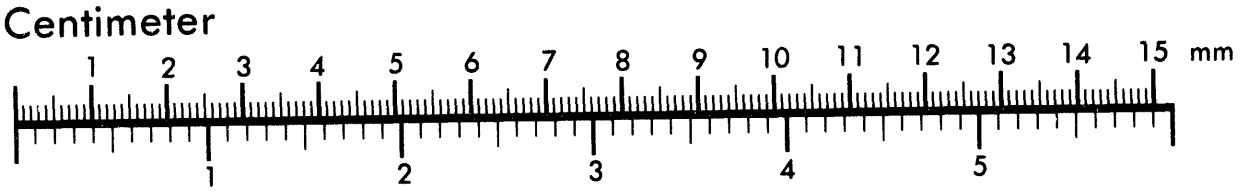

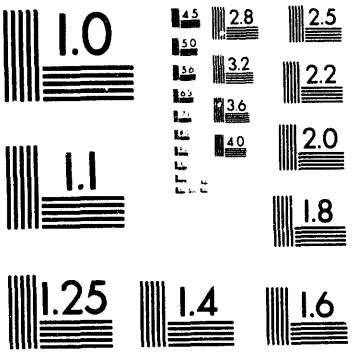

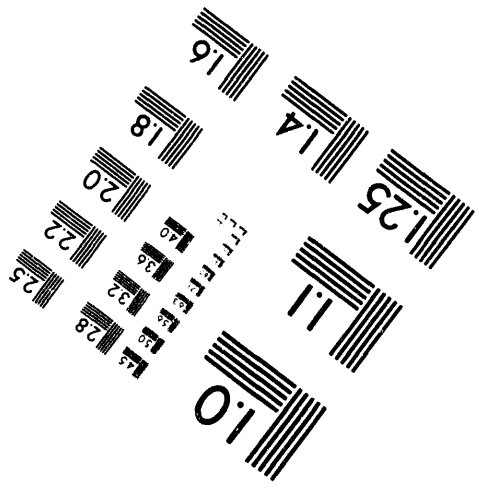

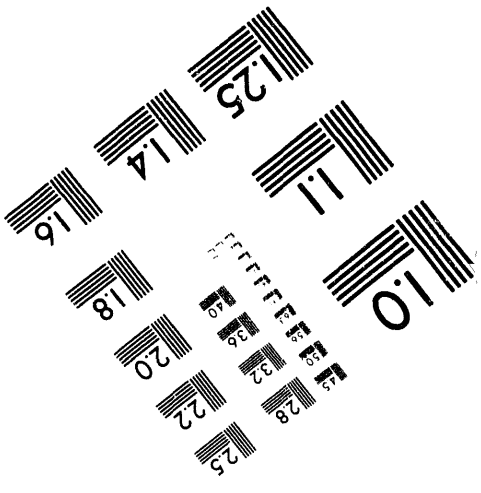

1 of 1

ANL/CHM/CP--83910
Conf-9408150--1

SPUTTERING OF TIN AND GALLIUM-TIN CLUSTERS*

Th. Lill, W. F. Calaway, Z. Ma, and M. J. Pellin

Materials Science, Chemical Technology, and Chemistry Divisions
Argonne National Laboratory
Argonne, Illinois 60439

Submitted for publication in the
Proceedings of the Tenth International Workshop
on Inelastic Ion-Surface Collisions
Grand Targhee Resort, Wyoming

August 8-12, 1994

*Work supported by the U.S. Department of Energy, BES-Materials Sciences, under Contract W-31-109-ENG-38.

Sputtering of tin and gallium-tin clusters

Th. Lill, W. F. Calaway, M. J. Pellin

Materials Science, Chemical Technology, and Chemistry Divisions

Argonne National Laboratory

Argonne, IL 60439

ABSTRACT

Tin and gallium-tin clusters have been produced by 4 keV Ar^+ ion bombardment of polycrystalline tin and the gallium-tin eutectic alloy and analyzed by time-of-flight mass spectrometry. The sputtered neutral species were photoionized with 193 nm (6.4 eV) excimer laser light. Neutral tin clusters containing up to 10 atoms and mixed gallium-tin clusters $Ga_{(n-m)}Sn_m$ with $n \leq 4$ for the neutrals and $n \leq 3$ for the sputtered ionic species have been detected. Laser power density dependent intensity measurements, relative yields, and kinetic energy distributions have been measured. The abundance distributions of the mixed clusters have been found to be nonstatistical due to significant differences in the ionization efficiencies for clusters with equal nuclearity but different number of tin atoms. The results indicate that Ga_2Sn and Ga_3Sn like the all-gallium clusters have ionization potentials below 6.4 eV. In the case of Sn_5, Sn_6, GaSn and $Ga_{(n-m)}Sn_m$ clusters with $n=2$ to 4 and $m>1$, we detect species that have sufficient internal energy to be one photon ionized despite ionization potentials that are higher 6.4 eV. The tin atom signal that is detected can be attributed to photofragmentation of dimers for both sputtering from polycrystalline tin and from the gallium-tin eutectic alloy.

1. Introduction

Cluster emission during ion bombardment of solid and liquid metal surfaces has become the object of intense investigation over the last few years. There are several reasons for this increased interest in metal cluster sputtering. First, the ejection mechanism for clusters appears to be different from that of atomic species. The linear collision cascade model (1, 2, 3) that has been proven to describe atom sputtering very satisfactorily, has only limited applicability to cluster sputtering (4). Therefore, the study of cluster sputtering is anticipated to provide new insights into sputtering, a key process in many leading edge technologies. Second, sputtered metal clusters have been found to play a significant role in laser secondary-neutral-mass-spectrometry of metal thin film interfaces (5, 6). and semiconductor materials (7). Third, cluster sputtering could find important applications in material science, for instance for the growth of nanomaterials.

Until recently, most of the information about sputtered clusters was based on ion cluster experiments, even though most clusters are ejected in the neutral state (8). These species have to be ionized prior to detection. Recently photoionization by means of UV lasers combined with very sensitive detection techniques led to a breakthrough in the experimental accessibility of large sputtered neutral metal clusters. Thus, clusters as large as Cu_{20} (9), Ag_{18} (8), Al_{12} (10), In_{32} (11), Ga_{14} (12) and mixed clusters $Ga_{(n-m)}In_m$ with $n \leq 10$ (13) and $Ga_{(n-m)}Al_m$ with $n \leq 14$ (14) have been detected. Relative cluster yields and kinetic energy distributions have been measured for these clusters.

The mixed cluster experiments have revealed new and unique information about the sputtering process including the depth of origin of clusters (13, 14). An increasing depth of origin was found for increasing cluster size in sputtering experiments on the liquid gallium-indium and gallium-aluminum eutectic alloys (13). While 94% of the sputtered atoms originate from the first atomic layer when the gallium-indium eutectic alloy is bombarded with 4 keV Ar^+ ions, only 68% of the atoms comprising clusters containing 8 atoms come solely from this outermost layer. The observation of statistical abundance distributions of the mixed gallium-indium and gallium-aluminum clusters was crucial for deriving information about the depth of origin of metal clusters from the experimental

data. It has been proposed that statistical abundance distributions can be observed, if chemical effects play a minor role and photoionization probabilities for all species are nearly equal. Since aluminum, gallium and indium are located in the same column of the periodic table of elements and atoms as well as clusters of these elements are one photon ionizable using an ArF-excimer laser, these conditions were fulfilled in the previous experiments.

This is not the case for the gallium-tin system reported herein. Since gallium is a group IIIA and tin a group IVA element, chemical effects likely play a role in the mixed system. The ionization potential (IP) of tin atoms is 7.34 eV and hence exceeds the photon energy of the available laser light (6.4 eV). Furthermore, ionization potentials that are higher than 6.4 eV have been reported for internally cold Sn_n clusters up to a nuclearity n=6 (15). The aim of this paper is to demonstrate that our conclusions regarding cluster sputtering obtained from experimental results for the gallium-indium and gallium-aluminum eutectic alloys are more general and can be applied to the more complex gallium-tin system. Emphasis will be put on the photoionization process. Key questions, this paper is concerned with, are: (i) the changes in the ionization efficiencies for subsequent substitution of gallium atoms with tin atoms for clusters with a given nuclearity, (ii) the influence of the internal energy of the sputtered clusters on the photoionization process, (iii) the relevance of relative cluster yield measurements for tin when 6.4 eV photons are used, and (iv) the influence of photofragmentation processes on kinetic energy distribution measurements for sputtered tin atoms and clusters.

2. Experimental

The experiments have been performed in the SARISA IV instrument developed in this laboratory and described in detail elsewhere (16). This ultra high vacuum apparatus is equipped with an angle- and energy-refocussing time-of-flight mass spectrometer especially designed for high detection efficiencies of photoionized particles. For sample preparation, pure gallium ingots and tin foil (ÆSAR) were used. The gallium-tin eutectic alloy (8.5 at.% Sn) was prepared by dissolving the proper amount of granular tin (Mallinckrodt) in molten gallium at about 100 °C overnight. The experiments have been performed near room

temperature, where the gallium-tin eutectic alloy is liquid (melting point 20.5 °C). As in the experiments with the gallium-indium and gallium-aluminum eutectic alloys, a piece of cobalt was used to support the liquid sample vertically in the instrument (13).

The samples were bombarded with 4 keV Ar^+ ions at normal incidence, the ion current being about 3 μA and the beam diameter at the sample about 300 μm. The SARISA IV instrument allows measurements of either sputtered neutral or ionized particles. The primary ion pulse length is chosen to be different for both modes. We used 160 ns and 2000 ns when detecting sputtered ions and neutrals, respectively (12). The ion pulse width is kept small in the secondary ion mode to achieve sufficient mass resolution, while in the secondary neutral mode the mass resolution is defined by the laser pulse width (typically 25 ns). The larger ion pulse width in the secondary neutral mode gains signal intensity since the ionization volume can be completely filled with species that represent the true velocity distribution. In other words, a long primary ion pulse duration is necessary for correct velocity integrated measurements of the sputtered neutrals.

In order to clean target surfaces, a continuous argon ion beam was rastered over a surface area of approximately 2 mm x 2 mm. The samples were cleaned for 1 to 2 hours before every experimental session. No sputter cleaning was necessary between single experimental runs as revealed by comparing spectra taken from the freshly rastered surface and from surfaces that have been kept in the vacuum chamber for several minutes without rastering.

The sputtered neutral atoms and clusters were ionized with 193 nm light from an ArF (6.4 eV) excimer laser that intersected the sputtered particle flux about 1 mm above the target surface with a cross section of 1 mm width and 2 mm height. Laser power dependent measurements have been performed by attenuating the laser beam with up to 7 partially absorbing quartz plates. Thus the laser power density could be varied in a range between 0.05 to 3 MW/cm^2.

By changing the delay time between when the ion puise struck the sample surface and when the laser pulse ionized the neutrals, distributions of the flight times of the sputtered species could be measured. This procedure is described

in detail in Ref. (9). In these experiments the distance between the sample surface and the midpoint of the cross section of the laser beam was 6 mm. The pulse duration was shortened to 200 ns and the laser cross section was decreased to 0.1 mm x 2 mm in order to provide well defined start conditions. It has been shown for this experimental arrangement that the intensity - flight time distributions can be transformed into flux - velocity and flux - kinetic energy distributions (9).

3. Results and discussion

A typical composite mass spectrum of sputtered neutrals from a polycrystalline tin surface and postionized at a laser power density of about 0.3 MW/cm^2 is shown in Fig. 1. Tin clusters up to Sn_{10} are clearly visible. The scaling factors reflect the rapid decrease of the cluster intensity with increasing cluster size. The rate of change of the cluster yield varies throughout the distribution. In particular, there is only a weak intensity change when comparing dimers and trimers. The relative cluster intensities will be discussed in more detail below.

Ion bombardment of the gallium-tin eutectic alloy leads to the ejection of all-gallium and all-tin clusters as well as mixed clusters making the spectrum more complex. Therefore in Figs. 2 and 3, the mass spectra are split into parts showing clusters with equal nuclearity separately. Figure 2 depicts mass spectra of the neutral atoms and clusters, which have been postionized at a laser power density of 1 MW/cm^2. Clusters containing up to 4 atoms are presented, although very low pentamer signals have also been detected. The atom and dimer spectra are dominated by the all-gallium species. Among the trimers and tetramers, the most intense peaks belong to Ga_2Sn and Ga_3Sn, respectively. At a first glance, gallium seems to be the major constituent at the surface of the gallium-indium eutectic alloy. Thermodynamics calculations predict, however, a strong tin surface segregation with a concentration of 87 at. % tin in the first atomic layer. Such a surface segregation of the minor constituent is known in the gallium - indium system (13, 17, 18, 19), where the indium surface concentration was measured to be 94 at. %.

There is evidence that tin is surface segregating from the spectrum in Fig. 2. For the dimers, for instance, an uniform tin concentration of 8.5 at. % for the bulk and the surface would result in an 116 - fold stronger Ga_2 intensity compared to Sn_2 (assuming a statistical formation process and equal photoionization efficiencies). This is an order of magnitude more than observed in the experiment. In Fig. 2, the abundance distributions of the clusters with equal nuclearity are clearly not statistical. The measured photoion intensities drop significantly for clusters containing equal numbers of tin and gallium atoms and for clusters in which tin atoms are the majority. Thus, for the trimers, there is a distinct intensity drop when going from Ga_2Sn to $GaSn_2$. For the tetramers, the measured intensity decreases gradually from Ga_3Sn to Ga_2Sn_2 and to $GaSn_3$.

The question arises as to what extend the departure from a statistical behavior is caused by chemical bonding differences and/or ionization efficiency variations. We have strong reason to believe, that differences in the ionization efficiencies play a major role here. (i) The gallium atoms (IP=6.0 eV) and all sputtered gallium clusters are one photon ionizable (12). In contrast, tin atoms and internally cold tin clusters containing up to 6 atoms are reported to be not one-photon ionizable with 6.4 eV photons (15). (ii) In laser vaporization experiments, statistical as well as nonstatistical combinations of component elements have been found for mixed clusters (20, 21, 22, 23, 24). For mixed clusters composed of group IVA - group VA and group IIIA - group VA metal combinations, the valence-electron-counting model, the so called "Wade's rules" (25), predict the pattern of the observed nonstatistical distributions. In this model, cluster bonding involves only p orbitals, and a cluster with nuclearity n has a stable bonding for configurations of $2n$+2, $2n$+4, or $2n$+6 p-electrons. As can easily be shown, for the group IIIA - group IVA system studied in our sputtering experiments, these configurations do not exist and therefore particular stable clusters are not expected. Furthermore, gallium and tin form an alloy in the bulk. Therefore the tendency to produce statistical distributions of mixed clusters would be anticipated. (iii) Further evidence for the decisive role of the ionization process comes from the cluster ion distributions shown in Fig. 3. Here, the abundance distributions for the dimers and trimers differ dramatically from those of the photoionized sputtered neutral clusters shown in Fig. 2. Thus, for the Ga_2Sn cluster, the measured photoion signal is larger than that of Ga_3, but in the secondary ion mode the Ga_2Sn signal is only about 25 %

compared to the all gallium trimer. The $GaSn_2$ and Sn_3 ion clusters signals were very low, and therefore, are not visible in the mass spectrum in Fig. 4. These observations can readily be explained by the exponential dependence of the secondary ion signal on the ionization potential of the atom (26) or cluster (8). From the comparable secondary ion intensities of the Ga_3 and Ga_2Sn clusters, it becomes clear that they should have similar IP within a few tens of an electron-volt (estimated less than 0.3 eV) and that there is a significant change in the IP when going to $GaSn_2$ and Sn_3. Since Ga_3 can be ionized with one 6.4 eV photon, it is very likely that this is also the case for Ga_2Sn. For $GaSn_2$ and Sn_3 a significant larger ionization potential is expected. For the tetramers, the secondary ion intensities are unfortunately very low. The high photoion signal intensity for Ga_3Sn suggests however that this cluster also has an IP below 6.4 eV. We note, that for sputtered neutral and ionic gallium - indium clusters, nearly identical abundance distributions have been found (13).

To estimate the tin concentration of the first atomic layer of the liquid gallium-tin alloy, we assume that the observed departures of the measured abundance distributions from the statistical picture are mainly caused by significant variations of the photoionization efficiencies for different species. Furthermore we assume that Ga_3Sn is, like Ga_4, one photon ionizable and that the measured intensities therefore reflect the true concentrations in the neutral flux. Using a binomial distribution as described in Ref. (12, 13), the tin concentration of the volume from where the tetramers are ejected (the *effective* tin concentration) is calculated from the Ga_4 and Ga_3Sn intensities to be about 55 at. %. Based on the experimental result that the fraction of sputtered atoms from the first atomic layer comprising neutral tetramers is 85 % for the gallium-indium system (12), we estimate the tin concentration of the first atomic layer for the gallium-tin system to be approximately 60 at. %. Thus, the experimental data indeed confirm the theoretical prediction of strong tin surface segregation. Using the effective tin concentration one can now estimate the relative Ga_2Sn_2, $GaSn_3$ and Sn_4 concentrations in the neutral flux. It turns out, that for laser power densities between 0.06 and 3 MW/cm^2 the ionizability of Ga_2Sn_2, $GaSn_3$ and Sn_4 are 4.3, 9.9 and 6.4 times, respectively, lower than for Ga_4 or Ga_3Sn.

The tin surface concentration as derived from the experimental results under the above assumptions is significantly lower (about 60%) than predicted by theory

(87 %). An eight times lower photoionization efficiency of Ga_3Sn compared to Ga_4 in our measurements would eliminate this discrepancy. Then, the ionization efficiencies for Ga_2Sn_2, $GaSn_3$, and Sn_4 would be 40, 330, and 700 times smaller than for Ga_4. The relevance of these numbers depends, however, on the accuracy of the calculations and will be viewed in the following as an upper limit.

Photoion signals have been measured as a function of laser power density in order to obtain more information about the ionizability of tin and mixed gallium-tin clusters with 6.4 eV photons. Fig. 4 depicts the results of a power study for clusters containing up to 4 atoms sputtered from polycrystalline tin. Similar data have been obtained for tin atoms and all-tin clusters sputtered from the gallium-tin eutectic alloy. The tin atom data follow closely a line with the slope of 2 on a log - log plot of the photoion signal intensity versus laser power density. This indicates a two-photon ionization process. As will be shown below, however, the atomic photoions originate almost exclusively from photofragmentation of tin dimers. For the dimers and trimers the slope is less than one for laser power densities below 1 MW/cm^2 and for higher values the photoion signal saturates and starts to decrease. This behavior does not necessarily indicate a single photon process. A two photon process can give similar results when photofragmentation processes are significant or when there is a resonance transition accessed.

A more valid criterion for single photon absorption is that relative ion intensities do not change for low laser power densities (15), especially when they are compared to a cluster that is known to be one photon ionizable. Fig. 5 shows the photoion intensities of the Ga_2Sn, $GaSn_2$ and Sn_3 clusters normalized to the one photon ionizable Ga_3 cluster as a function of the laser power density. For all three species, the dependences are week (note that the x-axis is logarithmic). The relative intensity of Ga_2Sn is nearly constant for laser power densities up to 0.5 MW/cm^2 and decreases by a factor of 1.5 when the laser power density is further increased by an order of magnitude. For $GaSn_2$ and Sn_3, the relative ion intensities decrease very slowly over the entire range of laser power densities. Similar dependences have been found for all tetramers.

A typical cross section for a two-photon process lies in the order of 10^{-30} cm^4 W^{-1} $molecule^{-1}$ (27). For indium atoms, a one-photon cross section of $8x10^{-17}$ cm^2 $atom^{-1}$ is reported (28). For laser power densities of 10^4 to 10^6 W/cm^{-2}, we would therefore expect signal intensities that are lower by many orders of magnitude for clusters that are two-photon ionized when compared to one photon ionizable clusters. In our experiment, the ionization efficiency for mixed gallium-tin tetramers containing more than one tin atom is lower by a factor 5 to 10 compared to Ga_4 or Ga_3Sn when assuming that the measured Ga_4 and Ga_3Sn photosignals reflect the concentration in the neutral flux. These numbers would exclude a two photon ionization process for any detected gallium-tin tetramer. As mentioned above, calculations based on the theoretical value for the surface tin concentration predict that the measured photoion signals of the tin containing clusters are 8 (for Ga_3Sn) to 700 times (for Sn_4) lower than in the neutral flux. Thus, even for this upper limit of the surface tin concentration, we obtain the result that Ga_3Sn should certainly be one photon ionizable. Since the photoion signals of all tetramers containing more than one tin atoms behave similar to the one-photon ionizable Ga_4 cluster when the laser power density is changed over almost two orders of magnitude (see Fig. 5), we exclude a two-photon ionization process for these clusters too.

We, therefore, conclude that all sputtered gallium-tin clusters that we have detected are mainly one-photon ionized and that the internal energy provided by the sputtering process is sufficient to allows this process. It is reasonable that the internal energies of sputtered clusters are significant. Recent molecular dynamics (MD) simulations on sputtered silver clusters revealed an internal energy content of roughly 1 eV per constituent atom (29). Unimolecular decomposition on a time scale of several tens of picoseconds after the ejection results in fragments that are internally colder than nascent clusters but certainly contain more internal energy than clusters produced in a pulsed nozzle source. We believe, that in the case of $GaSn_2$, Sn_3, Ga_2Sn_2, $GaSn_3$, and Sn_4, we detect clusters that have sufficient internal energy to be one-photon ionized. Their lower intensities compared to Ga_3, Ga_2Sn, Ga_4, and Ga_3Sn observed in the experiment can be attributed to the fact that we probe only the high energy portion of the internal energy distribution. According to the Franck-Condon principle for vertical transitions from vibrationally excited states (30), small

overlap integrals for transitions with small energy changes would cause further lowered intensities.

Figure 6 shows a log - log plot of the relative yields for clusters sputtered from polycrystalline tin, which have been ionized with different laser power densities, as a function of cluster nuclearity. As first demonstrated in Ref. (4) for aluminum and copper clusters, the yields of sputtered neutral and ionic clusters show a power law dependence on cluster nuclearity. As visible in Fig. 6, the relative intensities of tin clusters containing more than three atoms can also be fit by a power law. The slopes are -9.0, -9.5, -9.3, and -8.6 for laser power densities of 1.9, 1.1, 0.7, and 0.3 MW/cm^2, respectively. Thus, the slope of the power law appears to be independent of the laser power density used for photoionization. An average value of -9.1 $\pm$ 0.4 has been determined. The values of the relative cluster yields, however, are laser power density dependent. They decrease with increasing laser power density due to the quadratic tin atom intensity dependence on the laser power density (see Fig. 4).

We believe that the measured power law slope is similar to the value that would be obtained if the entire cluster yields were measured (i.e., if the cluster photoion signals were saturated without fragmentation) for the following reasons. First, the relative intensities of the Sn_7 and Sn_8 clusters, which have been reported to have IP's below 6.4 eV when generated in a pulsed nozzle source, lie nicely on the power law fits. This result supports our conclusion that a significant part of the sputtered tin trimers and tetramers has sufficient internal energy to be one-photon ionized and extends this finding to clusters containing five and six tin atoms. Second, the observed slope is in very good agreement with results on other materials. In previous studies, a linear dependence of the power law exponent on total sputtering yield was identified (4). The value for tin falls on this linear dependence and is very close to the value for aluminum. For aluminum, the total sputtering yield is 3.0 for 4 keV Ar^+ ion bombardment and the slope of the power law dependence was found to be -9.3. For tin, the sputtering yield is 2.5. Therefore the obtained slope of -9.1 is reasonable.

In certain cases, more information about photoionization and photofragmentation processes can be obtained from the velocity distribution of sputtered atoms and clusters (5, 6, 31, 32). For instance, it was observed that for

nonresonant multiphoton ionization of sputtered copper and aluminum species in the laser power density regime up to at least 10^8 W/cm^2, the atom signal detected is due to photofragmentation of dimers (31). This conclusion was based on the observation that the measured atomic velocity distributions peaked at the same velocity as the respective dimer distributions. Fig. 7 shows kinetic energy distributions of tin atoms sputtered from polycrystalline tin and ionized at two different laser power densities, 0.14 and 1.40 MW/cm^2. Both distributions are nearly identical and peak at about 1 eV. According to the linear collision cascade theory, the peak of the kinetic energy distribution is predicted to be located at $U/2$, with U being the surface binding energy, which is often equated to the heat of sublimation of the material. For tin, the bulk sublimation energy is 3.16 eV (33), i.e. $U/2$ is about 1.6 eV. The fact that the experimental value for $U/2$ is significantly lower than predicted by theory indicates that we may be detecting atoms that originated as dimers. In Fig. 7, the energy distribution of tin atoms sputtered from the gallium-tin eutectic alloy is plotted for comparison. This distribution is shifted towards even lower kinetic energies and peaks at about 0.5 eV.

The nearly identical distributions for tin atoms sputtered from polycrystalline tin and photoionized at low and high laser power densities as shown in Fig. 7 give strong evidence that those photoions are produced only by one process, either they represent two-photon ionized tin atoms or they are the result of tin dimer photofragmentation. The comparison of the atom and dimer velocity distributions reveals that the photofragmentation process is the source for the photoions. For a laser power density of 0.14 MW/cm^2, the atom and dimer velocity distributions peak at the same velocity. The velocity distribution of the dimers is slightly shifted to lower velocities for a laser power density of 1.4 MW/cm^2. The observation that the atomic photoions in multiphoton ionization of neutrals sputtered from polycrystalline tin are predominantly the result of tin dimer photofragmentation is in agreement with experimental results obtained by Husinsky, Nicolussi and Betz for sputtering of a polycrystalline aluminum-tin alloy (32).

The change of the kinetic energy distribution of the dimers with laser power density is illustrated in Fig. 8. For the higher laser power density, the data points are shifted towards lower kinetic energies. Several processes have to be

considered here. As shown in Ref. (31), the increasing amount of low energy dimers for increasing laser powers could be due to an enhanced photofragmetation of trimers. The assumption of a correlation between the internal and kinetic energy of the dimers (34) offers an additional explanation since either the ionization efficiencies and/or the fragmentation probabilities of the dimers could have different laser power dependences for species with different internal energies.

Finally, the dramatic difference in the kinetic energy distributions for neutral atoms sputtered from polycrystalline tin and from the gallium-tin eutectic alloy shall be discussed. The same effect has been observed for neutral indium atoms sputtered from polycrystalline indium and from the gallium-indium eutectic alloy. This was explained by considering the strong indium surface segregation for the alloy. In most cases, indium atoms are ejected from the surface after being struck by a gallium atom from below since gallium is the major bulk constituent. From momentum transfer considerations, there is less energy transferred to an indium atom from a collision with a gallium atom than from a collision with an indium atom. Since tin surface segregates in the gallium-tin eutectic alloy, the same argumentation can be applied here. Interestingly, the shift in the kinetic energy distribution is much stronger for the gallium-tin alloy compared to the gallium-indium alloy. Since we have found that tin atoms detected in the experiment are fragmented tin dimers, this could indicate that the tin dimers are sputtered as an entity since momentum transfer would be even less effective for gallium atom - tin dimer collisions.

Conclusions

Sputtering of neutral and ionic clusters under 4 keV Ar^+ ion bombardment from the gallium-tin eutectic alloy and of neutral tin clusters from polycrystalline tin has been studied. Neutral clusters as large as $Ga_{(n-m)}Sn_m$ with $n \leq 4$ and Sn_{10} as well as ionic clusters $Ga_{(n-m)}Sn_m$ with $n \leq 3$ have been detected. The gallium-tin eutectic alloy (tin bulk concentration 8.5 at.%) was found to be surface segregated, the tin concentration in the first atomic layer being at least 60 at. %. The abundance distributions of the sputtered neutral clusters ejected from the gallium-tin eutectic alloy and post-ionized with 6.4 eV photons are found to be

nonstatistical due to different photoionization efficiencies of the various clusters. Overall, substitution of gallium atoms by tin atoms leads to decreasing photoionization efficiencies for clusters of given nuclearity. Among the mixed clusters, Ga_2Sn and Ga_3Sn exhibit photoion intensities that indicate they are one-photon ionized with 6.4 eV photons. This is supported by secondary ion measurements. An estimate of the relative ionization efficiencies for the mixed and all-tin tetramers and laser power density dependent studies of the trimers and tetramers indicate that in the case of $GaSn_2$, Sn_3, Ga_2Sn_2, $GaSn_3$, and Sn_4, we mainly detect clusters that have sufficient internal energy to be one photon ionized. The relative cluster yield distributions for these clusters can be fit with a power law dependence, the slope δ being -9.3 $\pm$0.4, a value that lies on the general linear dependence of δ on the total sputtering yield which was discovered previously for a variety of metals. Finally, the measured neutral tin atom signal can be unequivocally attributed to be the result of the dimer photofragmentation process.

Acknowledgments

The authors would like to thank A. R. Krauss for calculations of the tin surface concentration in the gallium-tin alloy and K. R. Lykke for interesting and helpful discussions. This work was supported by the U.S. Department of Energy, BES-Material Sciences, under Contract W-31-109-ENG-38.

References

1. P. Sigmund, in: *Sputtering by particle bombardment I.* ed. by R. Behrisch, Springer, Berlin, Heidelberg, New York, 1981.

2. M. W. Thompson, *Philos. Mag.* **18** (1968) 377.

3. H. Oechsner, *Z. Physik* **238** (1970) 433.

4. S. R. Coon, W. F. Calaway, M. J. Pellin, J. M. White, *Surf. Sci.* **298** (1993) 161.

5. G. Nicolussi, W. Husinsky, G. Betz, *Phys. Rev. Lett.* **71** (1993) 1518.

6. G. Kampwerth, M. Terhorst, E. Niehuis, A. Benninghoven, in: *Secondary Ion Mass Spectrometry SIMS VIII* ed. by A. Benninghoven, K. T. F. Janssen, J. Tuempner, H. W. Werner, Wiley, Chichester, 1992.

7. S. W. Downey, A. B. Emerson, R. F. Kopf, *Nucl. Instr. and Meth. B* **62** (1992) 456.

8. A. Wucher, M. Wahl, H. Oechsner, *Nucl. Instrum. and Meth. B* **83** (1993) 73.

9. S.R. Coon, W.F. Calaway, M.J. Pellin, G.A. Curlee, J. M. White, *Nucl. Instrum. and Meth. B* **82** (1993) 329.

10. S.R. Coon, W. F. Calaway, J. W. Burnett, M. J. Pellin, D. M. Gruen, D. R. Spiegel, J. M. White, *Surf. Sci.* **259** (1991) 275.

11. Z. Ma, S. R. Coon, W. F. Calaway, M. J. Pellin, D. M. Gruen, E. I. von Nagy-Felsobuki, *J. Vac. Sci. Technol. A* **12** (1994) 2425.

12. Th. Lill, W. F. Calaway, Z. Ma, M. J. Pellin, *Surf. Sci.*, submitted.

13. Th. Lill, W. F. Calaway, M. J. Pellin, D. M. Gruen, *Phys. Rev. Lett.*, submitted.

14. Th. Lill, W.F. Calaway, M. J. Pellin, Proceedings of the Spring meeting of the AVS Illinois Chapter, Evanstone, 1994.

15. K. LaiHing, R. G. Wheeler, W. L. Wilson, M. A. Duncan, *J. Chem. Phys.* **87** (1987) 3401.

16. M.J. Pellin, C. E. Young, W. F. Calaway, J. W. Burnett, B. Jørgensen, E. L. Schweitzer, D. M. Gruen, *Nucl. Instrum. and Meth. B* **18** (1987) 446.

17. M.F. Dumke, T.A. Tombrello, R.A. Weller, R.M. Housley, E. H. Cirlin, *Surf. Sci.* **124** (1983) 407.

18. K.M. Hubbard, R.A. Weller, D.L. Weathers, T. A. Tombrello, *Nucl. Instrum. and Meth. B* **40** (1989) 278.

19. K.M. Hubbard, R.A. Weller, D.L. Weathers, T. A. Tombrello, *Nucl. Instrum. and Meth. B* **36** (1989) 395.

20. E. A. Rohlfing, D. M. Cox, R. Petkovic-Luton, A. Kaldor, *J. Phys. Chem.* **88** (1984) 6227.

21. M. B. Bishop, K. LaiHing, P. Y. Cheng, M. Peschke, M. A. Duncan, *J. Phys. Chem.* **93** (1989) 1566.

22. R. G. Wheeler, K. LaiHing, W. L. Wilson, J. D. Allen, M. A. D. R. B. King, *J. Am. Chem. Soc.* **108** (1986) 8101.

23. R. G. Wheeler, K. LaiHing, W. L. Wilson, M. A. Duncan, *J. Chem. Phys.* **88** (1988) 2831.

24. D. Schild, R. Pflaum, K. Sattler, E. Recknagel, *J. Phys. Chem.* **91** (1987) 2649.

25. K. Wade, *Adv. Inorg. Chem. Radiochem.* **18** (1976) 1.

26. M. L. Yu, in: *Sputtering by particle bombardment III.* ed. by R. Behrisch, Springer, Berlin, Heidelberg, New York, 1982.

27. K. R. Lykke, B. D. Kay, *J. Chem. Phys.* **95** (1991) 2252.

28. A. Wucher, Z. Ma, W.F. Calaway, M. J. Pellin, *Surf. Sci. Lett.* **304** (1994) L439.

29. A. Wucher, B. J. Garrison, *Phys. Rev. B* **46** (1992) 4855.

30. G. Herzberg, *Molecular spectra and molecular structure*, Van Nostrand Reinhold, New York, 1950.

31. S. R. Coon, W. F. Calaway, M. J. Pellin, J. W. Burnett, J. M. White, *Surf. Interface Anal.* **20** (1993) 1007.

32. W Husinsky, G. Nicolussi, G. Betz, *Nucl. Instr. and Meth. B* **82** (1993) 323.

33. *Handbook of Chemistry and Physics.*, ed. by R. C. Weast, CRC Press Inc., Boca Raton, Florida, 1988.

34. Z. Ma, W. F. Calaway, M. J. Pellin, E. I. v. Nagy-Felsobuki, *Nucl. Instrum. and Meth. B* , in press.

Figure captions

1. Typical mass spectrum of neutral clusters ejected from polycrystalline tin during 4 keV argon ion bombardment and postionized with 6.4 eV photons at a power density of 0.3 MW/cm^2. Portions of the spectrum are magnified by the indicated scaling factors.

2. Typical mass spectrum of neutral clusters ejected from the liquid gallium-tin eutectic alloy during 4 keV argon ion bombardment and postionized with 6.4 eV photons at a power density of 1 MW/cm^2. The four panels show mass peaks corresponding to clusters with equal nuclearity. The scaling factors are indicated.

3. Typical mass spectrum of positively charged clusters ejected from the liquid gallium-tin eutectic alloy during 4 keV argon ion bombardment. The three panels show mass peaks corresponding to clusters with equal nuclearity. The scaling factors are indicated.

4. Intensities of neutral tin clusters ejected from polycrystalline tin during 4 keV argon ion bombardment and postionized with 6.4 eV photons as a function of the laser power density. The dashed line indicates a quadratic dependence.

5. Intensities of neutral $Ga_nSn_{(3-n)}$ clusters for n=0 to 2 normalized to the intensity of the neutral Ga_3 cluster as a function of the laser power density used for postionzation with 6.4 eV photons. The clusters are produced by 4 keV argon ion bombardment of the liquid gallium-tin eutectic alloy. The circles represent the normalized intensity for the Sn_3 cluster, the triangles for the $GaSn_2$ cluster and the open square for the Ga_2Sn cluster.

6. Relative yields of neutral clusters sputtered from polycrystalline tin and postionized with 6.4 eV photons at 1.9 MW/cm^2 (circles), at 1.1 MW/cm^2 (triangles), at 0.7 MW/cm^2 (squares), and at 0.3 MW/cm^2 (diamonds) as a function of cluster nuclearity. The lines represent least square fits to a power law.

7. Kinetic energy distributions (flux versus kinetic energy) for neutral tin atoms sputtered from the gallium-tin eutectic alloy and postionized with 6.4 eV photons at 0.90 MW/cm^2 (solid line), and for neutral tin atoms from polycrystalline tin postionized at 1.40 MW/cm^2 (dashed line) and 0.14 MW/cm^2 (dotted line).

8. Kinetic energy distributions (flux versus kinetic energy) for neutral dimers sputtered from polycrystalline tin and postionized at 1.40 MW/cm^2 (circles) and 0.14 MW/cm^2 (triangles).

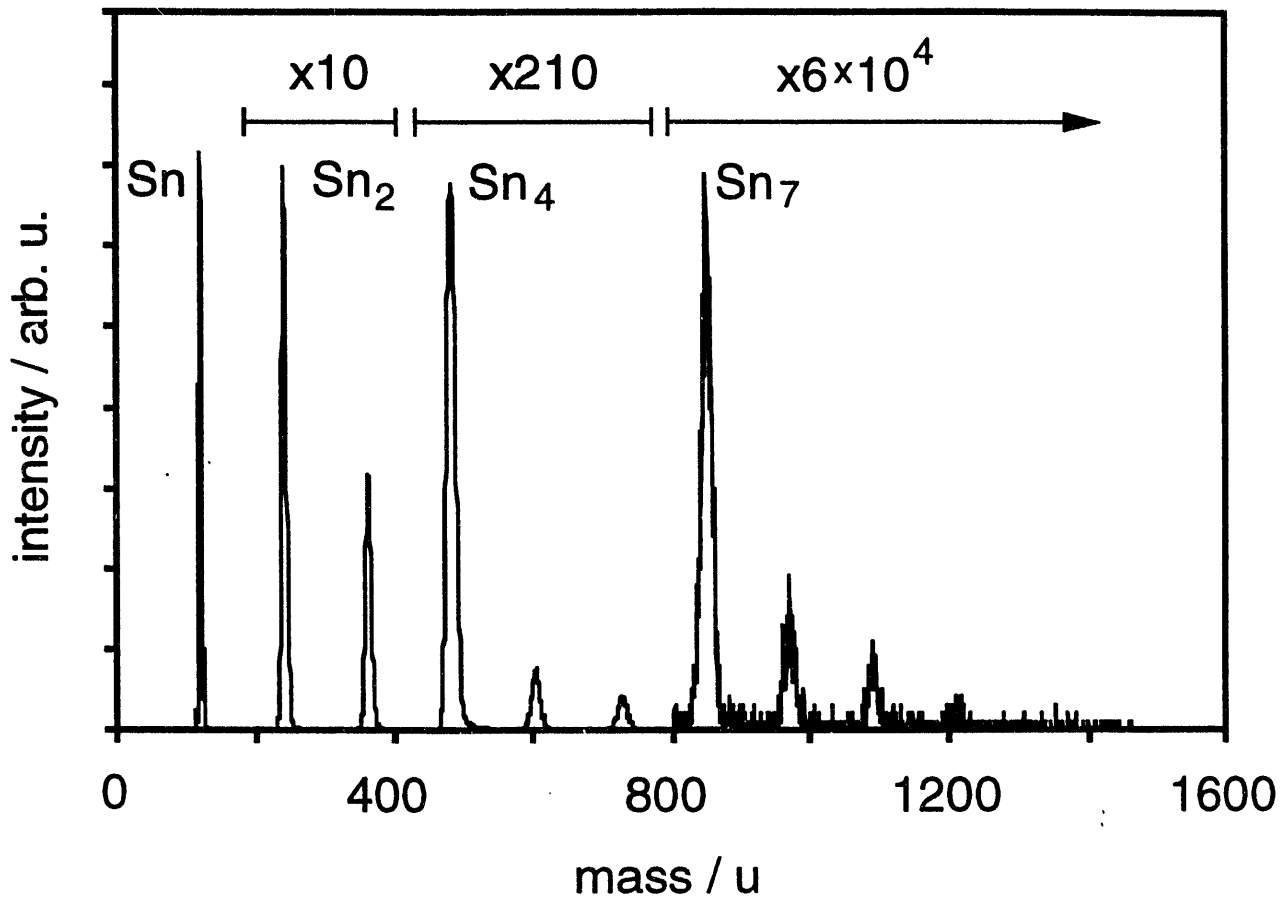

Lill, Calaway, Pellin

Fig. 1

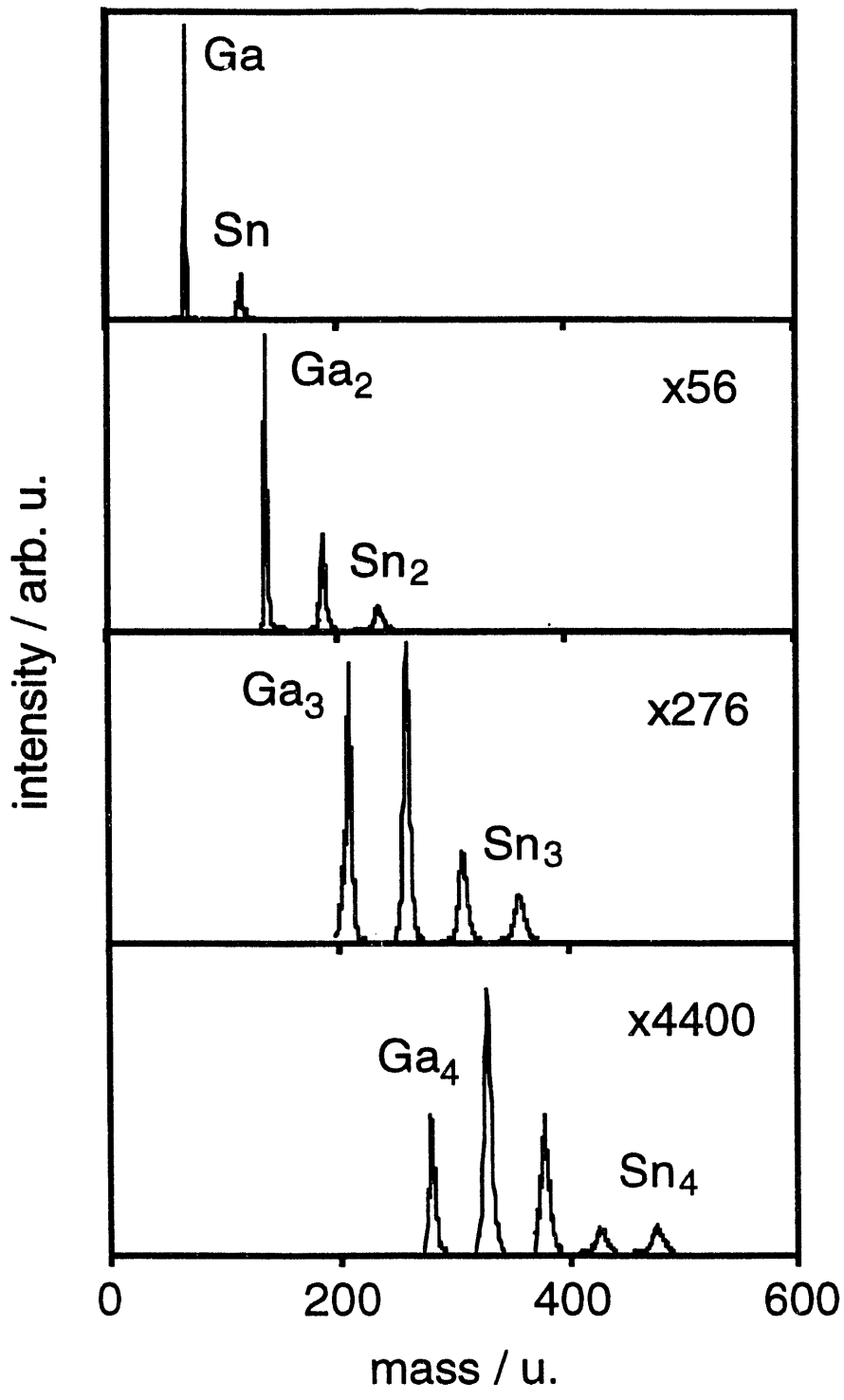

Lill, Calaway, Pellin

Fig 2

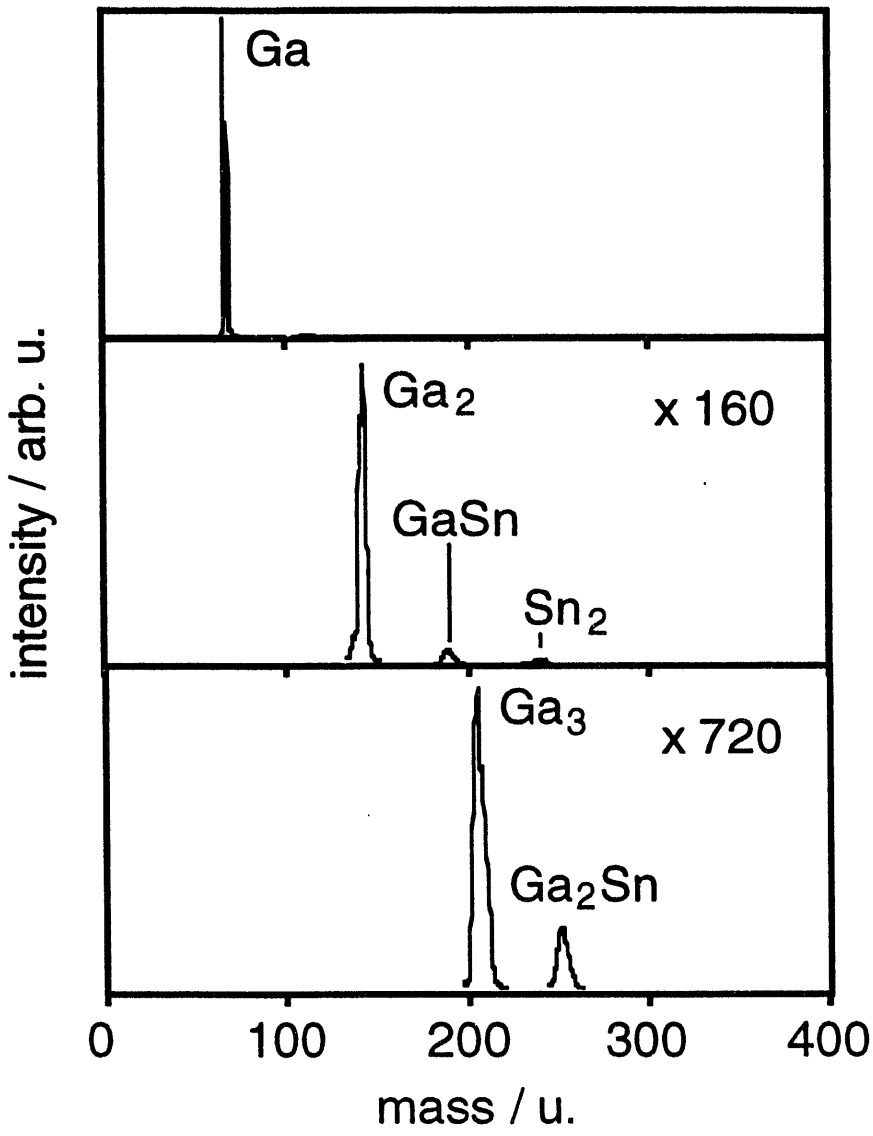

Lill, Calaway, Pellin

Fig 3

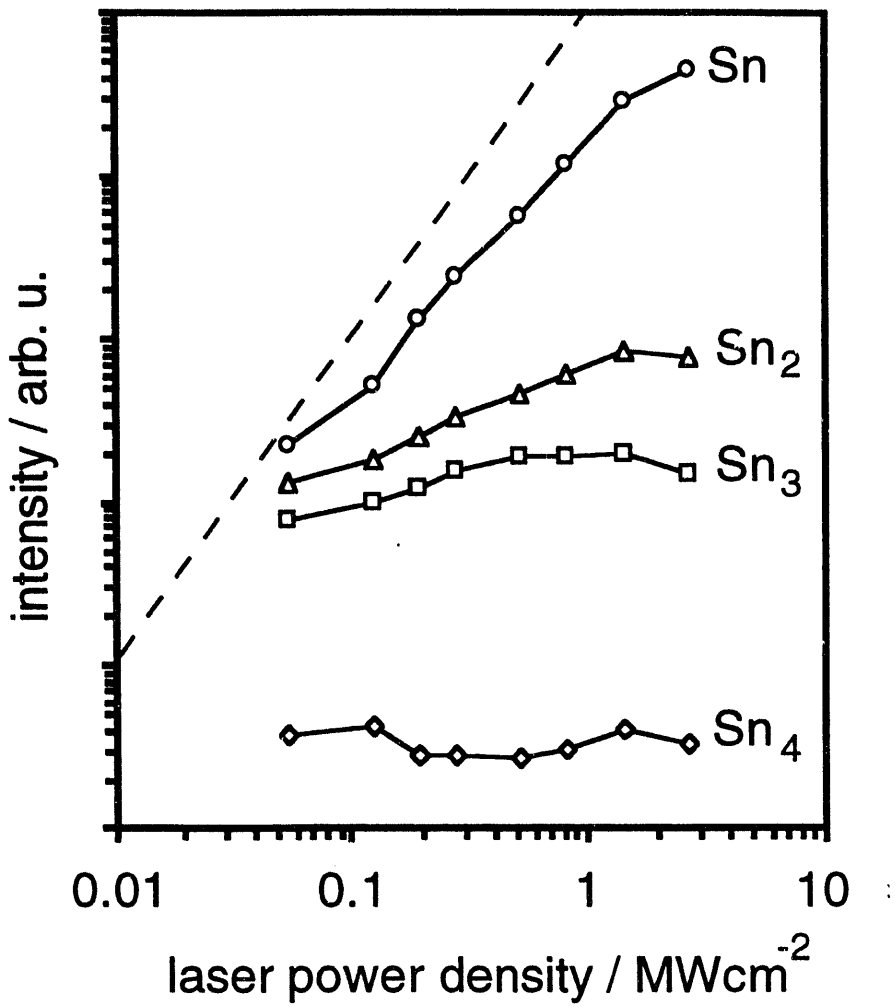

Lill, Calaway, Pellin

Fig 4

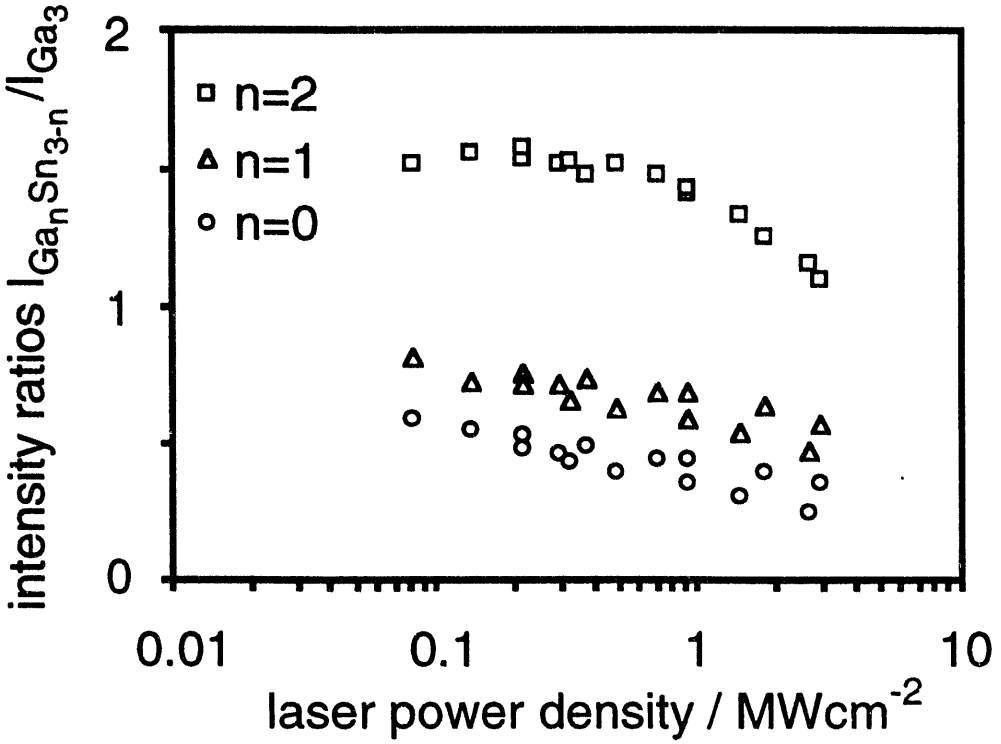

Lill, Calaway, Pellin

Fig. 5

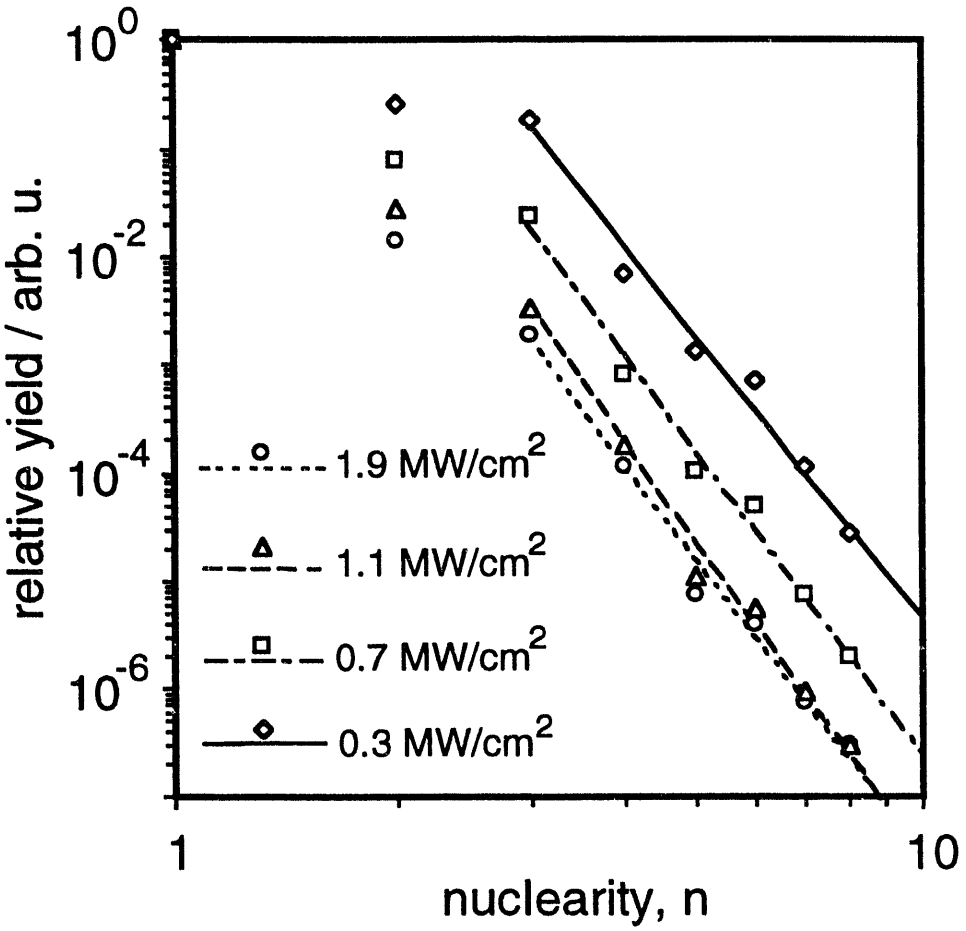

Lill, Calaway, Pellin

Fig 6

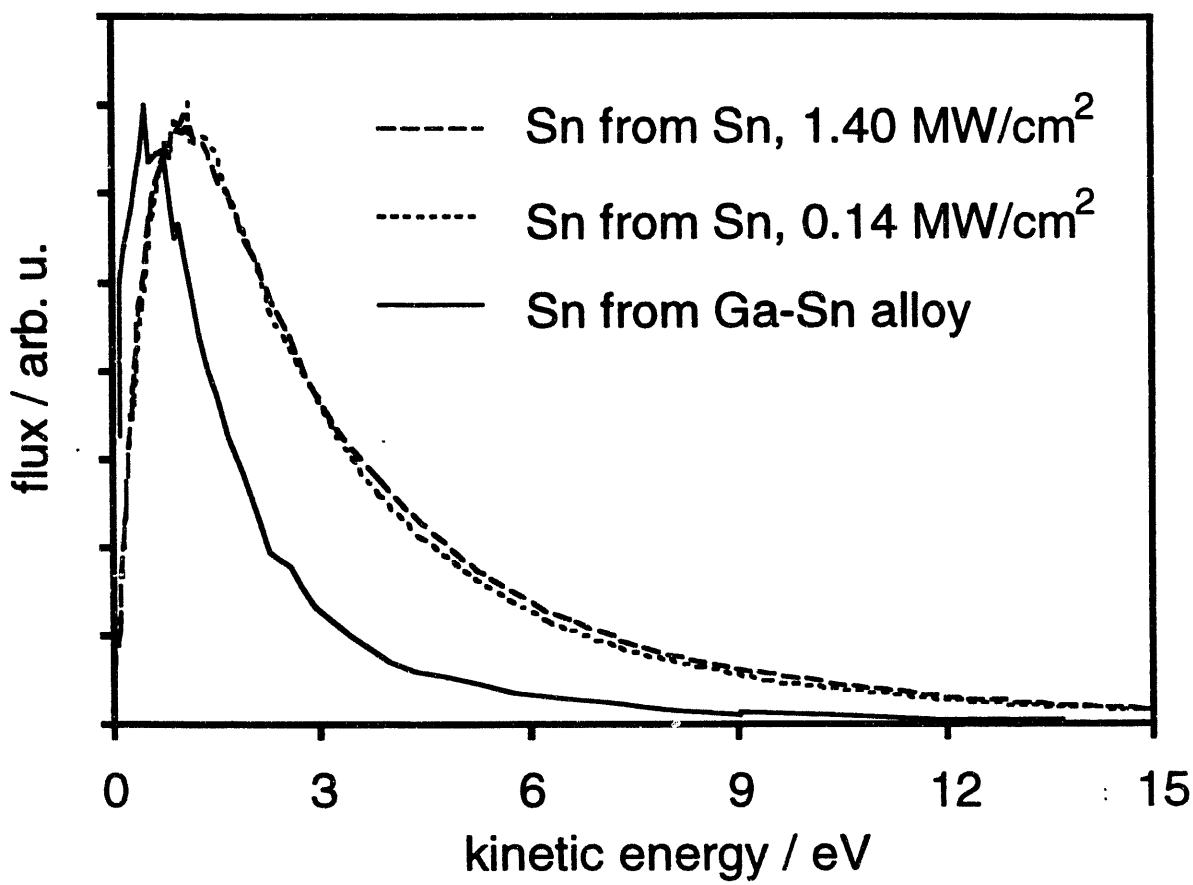

Lill, Calaway, Pellin

Fig 7

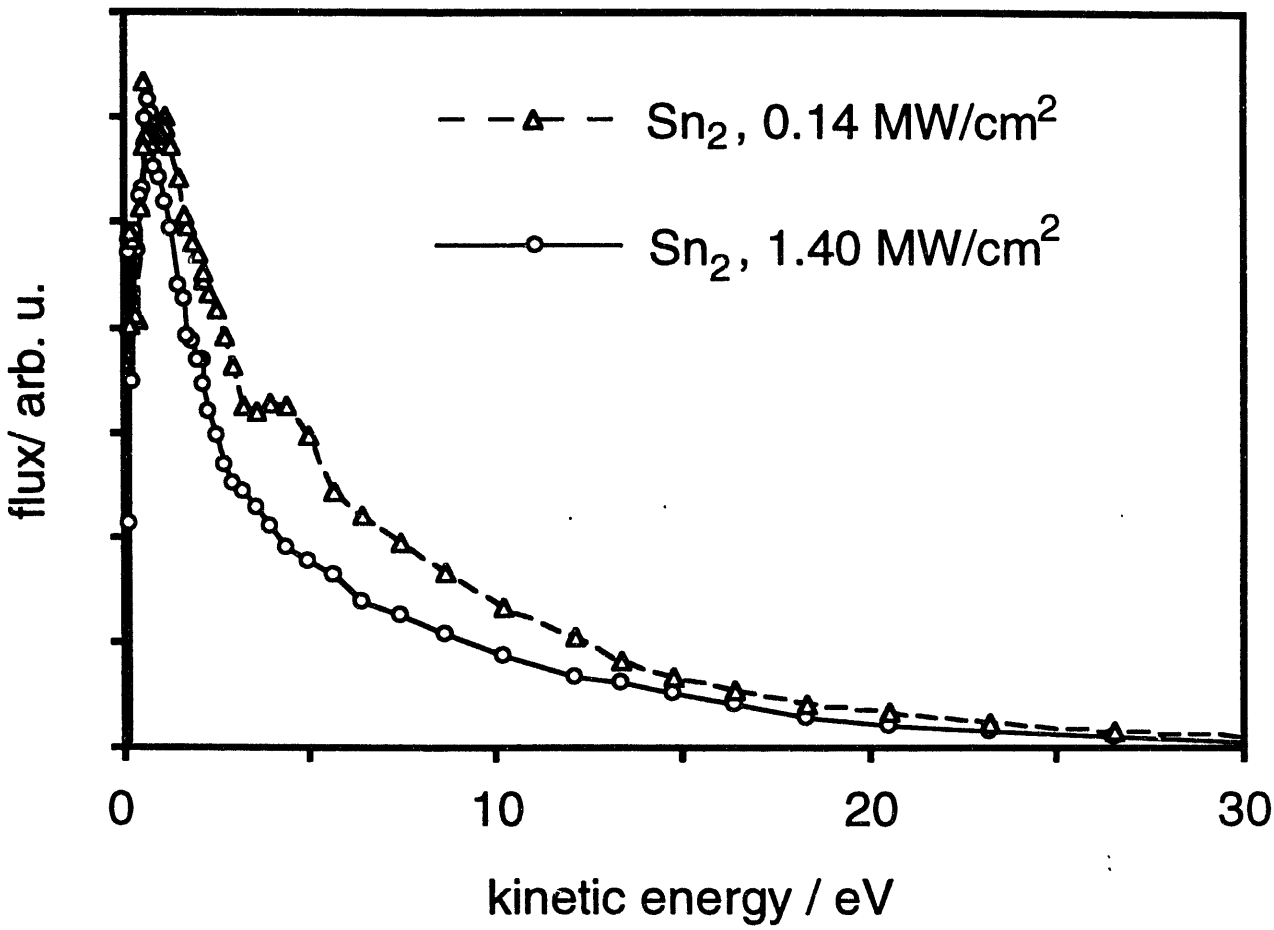

Lill, Calaway, Pelhi

Fig. 8

DATE
FILMED
10/18/94
END